

## Direct measurement of evanescent wave enhancement inside passive metamaterials

Bogdan-Ioan Popa\* and Steven A. Cummer

Department of Electrical and Computer Engineering, Duke University, Durham, North Carolina 27708, USA

(Received 22 June 2005; published 25 January 2006)

Electric-field measurements inside a negative-permeability-positive-permittivity metamaterial composed of arrays of split-ring resonators directly show that the theoretically predicted enhancement of evanescent waves in passive materials is physically realizable. To circumvent the extreme sensitivity of this phenomenon to the material parameters, we show how the basic phenomenon occurs under relaxed conditions for a single transverse wave number and use this approach in our measurements. Measurements of the spatial distribution of the electric field in a three-slab configuration confirm that the evanescent wave enhancement responsible for the subwavelength focusing effect occurs in an electromagnetic material in a manner in close agreement with theory.

DOI: [10.1103/PhysRevE.73.016617](https://doi.org/10.1103/PhysRevE.73.016617)

PACS number(s): 41.20.Jb, 78.20.Ci

Pendry [1] has shown, theoretically, that carefully designed negative index of refraction materials (NIMs) can be used to build flat lenses that can image objects arbitrarily small, thus, breaking the resolution limit imposed by the diffraction theory. As Pendry pointed out, there are two properties that enable NIM slabs to achieve this subwavelength focusing effect. First, there is the negative refraction predicted by Veselago [2], a property that was demonstrated through experiments involving NIMs made of arrays of wires and split-ring resonators (SRRs) [3,4]. The second and more surprising property, which allows surpassing the resolution limit of conventional lenses, is the evanescent wave recovery inside properly designed NIMs. More specifically, Pendry showed that evanescent waves in air can be exponentially enhanced inside a finite NIM slab with a relative permittivity and permeability equal to  $-1$ . Using a two-dimensional (2D) transmission line analog of a NIM, subwavelength focusing was demonstrated and attributed qualitatively to evanescent wave enhancement [5]. Fang *et al.* [6] have shown that a thin silver slab can transmit subwavelength information using an approach first suggested by Pendry [1]. More recently, Baena *et al.* [7] used an anisotropic SRR-made metamaterial in an experiment that demonstrated a greatly enhanced tunneling effect by showing transmission peaks at expected frequencies. This so-called perfect tunneling effect was again explained through the exponential growth of evanescent waves inside the metamaterial. It has yet to be shown directly, however, that evanescent wave enhancement occurs in these materials in the manner predicted theoretically.

In this paper, we present measurements of the spatial distribution of fields inside a metamaterial composed of SRRs that directly show the enhancement of evanescent waves inside the metamaterial. The measured fields are in close agreement with theoretical predictions, confirming the fundamental behavior of wave fields inside materials in the proper configurations that can produce evanescent wave enhancement and consequently subwavelength focusing.

An approach based on rf waveguides is used for controlled excitation of evanescent waves of known transverse wavenumber [7]. We use the following procedure to design and test an isotropic metamaterial that enhances, in a three slab configuration, the  $TE_{10}$  evanescent mode inside a rectangular metal waveguide operated below cutoff. The requirement that only one transverse wave number be enhanced simplifies the material design constraints, as shown below. Consider a three-slab configuration (air/metamaterial of thickness  $d$ /air) inside a metallic rectangular waveguide of width  $a$  and height  $b < a$ , as in Fig. 1. We obtain evanescent waves inside this waveguide by using a source situated at  $z_{\text{src}} < -d$  that operates below the cutoff frequency of the waveguide, i.e.,  $f < f_c = c/2a$ .

It has been shown theoretically [9,10] that small material parameter perturbations significantly limit the effect we wish to measure and that modes with smaller transverse wave numbers better tolerate these deviations. Consequently, since it has the lowest transverse wave number ( $\pi/a$ ) of all the modes in a given rectangular waveguide, we focus on measurements of the  $TE_{10}$  mode. Our straight-wire waveguide excitation dominantly excites  $TE_{m0}$  modes, and for reasons that are shown below, our metamaterial will predominantly have a magnetic response and thus will interact much more weakly with  $TM$  modes. We therefore limit the analysis that follows to  $TE_{mn}$  modes. The variation of the fields in the transverse,  $xy$  plane, is also neglected because all measurements will be performed along a line parallel to the  $z$  axis, for which  $x$  and  $y$  are constants.

We can find the analytical expressions of the fields inside

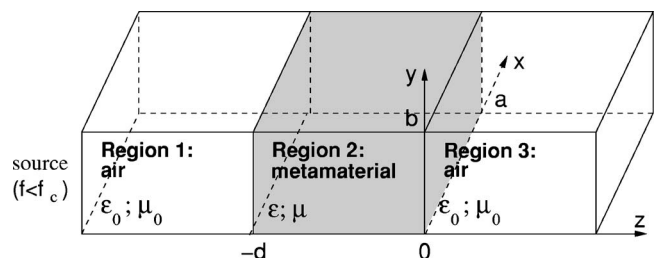


FIG. 1. Waveguide dimensions.

\*Electronic address: [bap7@ee.duke.edu](mailto:bap7@ee.duke.edu)

the three slabs considered using a procedure outlined in Ref. [14]. Thus, assuming an  $e^{+j\omega t}$  time dependence, the component of the electric field in the  $y$  direction in the three regions shown in Fig. 1 is given by  $E_i = A_i^+ e^{-\alpha_i z} + A_i^- e^{\alpha_i z}$ , where index  $i$  is the number of the region ( $i=1,3$ ),  $\alpha_i$  is the attenuation coefficient for the  $TE_{mn}$  mode in region  $i$ , ( $\alpha_1 = \alpha_3 = \alpha_0 \equiv \sqrt{(m\pi/a)^2 + (n\pi/b)^2 - \omega^2 \epsilon_0 \mu_0}$ ,  $\alpha_2 = \alpha \equiv \sqrt{(m\pi/a)^2 + (n\pi/b)^2 - \omega^2 \epsilon \mu}$ ), and  $A_i^+$  and  $A_i^-$  are constants that are to be determined. The terms  $A_1^- e^{\alpha_1 z}$  and  $A_2^- e^{\alpha_2 z}$  account for the reflections at the  $z=-d$  and, respectively,  $z=0$  boundaries ( $A_3^- = 0$  since the fields must be finite in the semi-infinite third region). We determine the constants  $A_i^+$  and  $A_i^-$  by imposing that the tangential electric and magnetic fields be continuous across the  $z=-d$  and  $z=0$  boundaries. For  $TE_{mn}$  modes, it follows that the  $y$  component of the electric fields inside the three regions can be written as

$$E_1 = C \frac{e^{d\alpha} - e^{-d\alpha}}{2\Delta} \left[ e^{-\alpha_0(z+d)} \left( 1 + 2 \frac{1 + e^{2d\alpha}}{-1 + e^{2d\alpha} \Delta + \Delta^2} \right) + e^{\alpha_0(z+d)} (\Delta^2 - 1) \right] \quad (1)$$

$$E_2 = C [e^{-\alpha z} (1 + \Delta) + e^{\alpha z} (1 - \Delta)] \quad (2)$$

$$E_3 = 2C e^{-\alpha_0 z}, \quad (3)$$

where  $C$  is a constant that depends on the source, and  $\Delta = \alpha_0 \mu / \alpha \mu_0$ .

A closer look at Eq. (2) shows that purely growing (in the  $+z$  direction) evanescent fields can be obtained inside the second region and purely decaying fields in the first region if  $1 + \Delta = 0$ , or equivalently

$$\mu = -\mu_0 \frac{\alpha}{\alpha_0} = -\mu_0 \frac{\sqrt{k_{mn}^2 - \omega^2 \epsilon \mu}}{\sqrt{k_{mn}^2 - \omega^2 \epsilon_0 \mu_0}} \quad (4)$$

where  $k_{mn} \equiv \sqrt{(m\pi/a)^2 + (n\pi/b)^2}$  is the transverse wave number corresponding to the  $TE_{mn}$  mode.

Note from Eq. (4) that, as Pendry predicted [1], in order to enhance every  $TE_{mn}$  mode, the metamaterial should have, simultaneously,  $\epsilon/\epsilon_0 = \mu/\mu_0 = -1$ . This is difficult to achieve in practice because the material must be tuned to have  $\epsilon/\epsilon_0$  and  $\mu/\mu_0$  to be extremely close to  $-1$  [9] at exactly the same frequency. Moreover, the wire medium frequently used to realize negative permittivity can be difficult to control in design and fabrication [4].

However, if we require only one mode (equivalently, one transverse wave number) to exhibit the same evanescent enhancement, the constraints on  $\epsilon$  and  $\mu$  are relaxed considerably. We assume for simplicity in the following that there are no losses, i.e.,  $\alpha$  and  $\alpha_0$  are real and positive. Consequently, Eq. (4) shows that the permeability of the required material has to be negative, i.e.,  $\mu < 0$ . It was demonstrated in both experiments [3] and theory [8] that an isotropic metamaterial composed of SRRs much smaller than the wavelength can be approximated by a homogeneous medium characterized by an effective permeability given by (we neglect losses for simplicity)

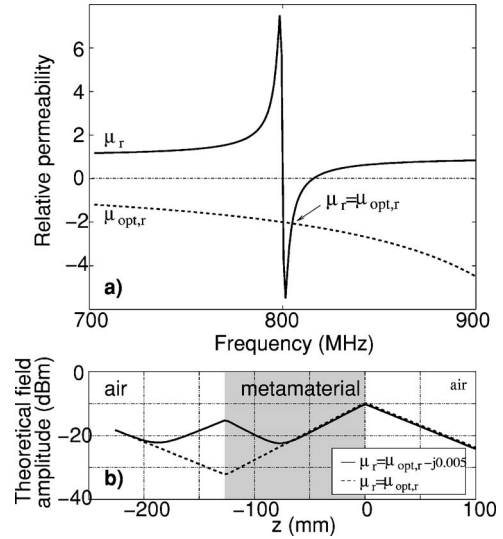


FIG. 2. (a) The relative optimal permeability and the relative permeability of an isotropic SRR metamaterial. The resonant frequency is 800 MHz; (b) the electric field ( $TE_{10}$  mode) for  $\mu_r = \mu_{\text{opt},r} - j0.005$  and  $\mu_r = \mu_{\text{opt},r} = -1.2664$ .

$$\mu = \mu_0 \left( 1 - \frac{f_p^2}{f^2 - f_0^2} \right) \quad (5)$$

where the plasma frequency,  $f_p$ , and the resonant frequency,  $f_0 \gg f_p$ , of the SRR material depend on the SRR geometry. As can be seen from Eq. (5), the effective permeability becomes negative in a narrowband above  $f_0$ . Moreover, it was also suggested [7] that below the cutoff frequency of the waveguide the SRR slab has a positive effective relative permittivity,  $\epsilon_r \equiv \epsilon/\epsilon_0$ , equal or slightly greater than 1. Since this effective permittivity is slowly varying with frequency [12], we can consider  $\epsilon$  constant in the narrowband where  $\mu < 0$ . Under these assumptions, we can now solve Eq. (4) to find the optimal relative permeability,  $\mu_{\text{opt}}$ , that produces evanescent wave enhancement of a single  $TE_{mn}$  mode inside the material:

$$\mu_{\text{opt}} = -\mu_0 \frac{0.5(\epsilon_r - A)(2\pi f/c k_{mn})^2 + A}{1 - (2\pi f/c k_{mn})^2}, \quad (6)$$

where  $A = \sqrt{1 + (\epsilon_r^2 - 1)/[2(c k_{mn}/2\pi f)^2 - 1]^2}$  is a number between 1 and  $\epsilon_r$ . Thus, enhancement of evanescent  $TE$  modes can only be achieved with a material with negative permeability. Note that, in general, the enhancement of each  $TE_{mn}$  mode requires a different permeability and will thus occur for a different frequency in an SRR medium.

For the reasons mentioned previously, we focus on the enhancement of the  $TE_{10}$  mode, for which  $k_{10} = \pi/a$ . A plot of  $\mu_r = \mu/\mu_0$  and  $\mu_{\text{opt},r} = \mu_{\text{opt}}/\mu_0$  for the  $TE_{10}$  mode as given by Eqs. (5) and (6) reveals that for every lossless isotropic metamaterial made of SRRs, there is always a frequency for which the evanescent  $TE_{10}$  mode is enhanced because the SRR material exhibits all negative values of  $\mu$  in a fairly narrow frequency band [see Fig. 2(a)]. Rather than design a material with a given  $\epsilon$  and  $\mu$  at a specific, predetermined

frequency, we can simply design a material with a resonant  $\mu$  response in the general frequency range of interest, knowing that at some frequency the conditions for evanescent  $TE_{10}$  mode wave enhancement will be met and that we can find this frequency experimentally. Real materials are lossy, and, as others have shown [4,9,10], the evanescent field enhancement property is very sensitive to loss. To roughly quantify how much loss can be tolerated, we consider the following numerical example. Consider a waveguide of width  $a = 8.6$  cm. Suppose that  $\epsilon_r = 1$ , and  $\mu_r = \mu_{\text{opt},r}$  at  $f_{\text{opt}} = 800$  MHz ( $\mu_{\text{opt},r} = -1.2664$  at 800 MHz). We use Eqs. (1)–(3) to plot the expected electric field inside this waveguide. The solid line in Fig. 2(b) represents the electric field if the relative permeability of the metamaterial is  $\mu_r = \mu_{\text{opt},r} - j0.005$  (i.e., slightly lossier than the optimal value), and as a reference, we also plot the fields in the ideal case when  $\mu_r = \mu_{\text{opt},r}$  (see the dotted line). As can be seen in Fig. 2(b), as long as the loss is reasonably low, only the fields at the first interface are perturbed from the ideal solution, and the enhancement of the  $TE_{10}$  mode is still as expected with the fields outside the metamaterial the same as if the metamaterial were lossless. On the other hand, deviations  $< 3\%$  from  $\mu_{\text{opt}}$  bring the level of the electric field more than 10 dB below that in the ideal case. This high sensitivity was also observed by others [9,10]. The question that emerges is how likely is it to build such a low-loss SRR metamaterial. A previous experiment involving an SRR-only-based metamaterial [7] suggested an effective permeability loss tangent of around 0.01–0.1, which, as we will shortly see, is low enough to allow significant growth of the evanescent  $TE_{10}$  mode, and also consistent with our results.

Our aim was to design an isotropic metamaterial made of SRRs, measure the electric field inside it, and compare it to that in Fig. 2(b). We used a straight section of an aluminium WR340 rectangular waveguide of width 8.6 cm and height 4.3 cm (the cutoff frequency of the  $TE_{10}$  mode is 1.74 GHz). The source consists of a straight wire oriented along the  $y$  axis. For this orientation, the wire excites dominantly  $TE_{m0}$  modes [13] (i.e., the modes for which the electric field is along the  $y$  axis, and the magnetic field has nonzero components in the  $x$  and  $z$  directions), other modes having negligible amplitudes. A 20 dB microwave amplifier is used at the source to boost the fields inside the waveguide and improve the signal-to-noise ratio.

We designed an SRR that would have a resonant frequency well below the cutoff frequency of the waveguide. By scaling the SRR described in Ref. [11], which had a resonant frequency  $\sim 2.6$  GHz, we obtained a SRR with a resonant frequency between 800–900 MHz. The geometry of the SRR can be seen in Fig. 3(a). Like in Ref. [11], the SRRs were fabricated on a low-loss TMM3 substrate. In order to make our metamaterial isotropic with  $\mu < 0$ , we arranged the SRRs to be perpendicular on the magnetic-field components of the  $TE_{m0}$  modes in both the longitudinal and transverse directions. A photograph of the metamaterial is presented in Fig. 3(b), and the top of Fig. 4 shows how the metamaterial was positioned inside the waveguide. Small holes drilled in the waveguide wall allowed us to measure the electric field inside the waveguide using a short wire probe. The position of these access holes relative to the SRR

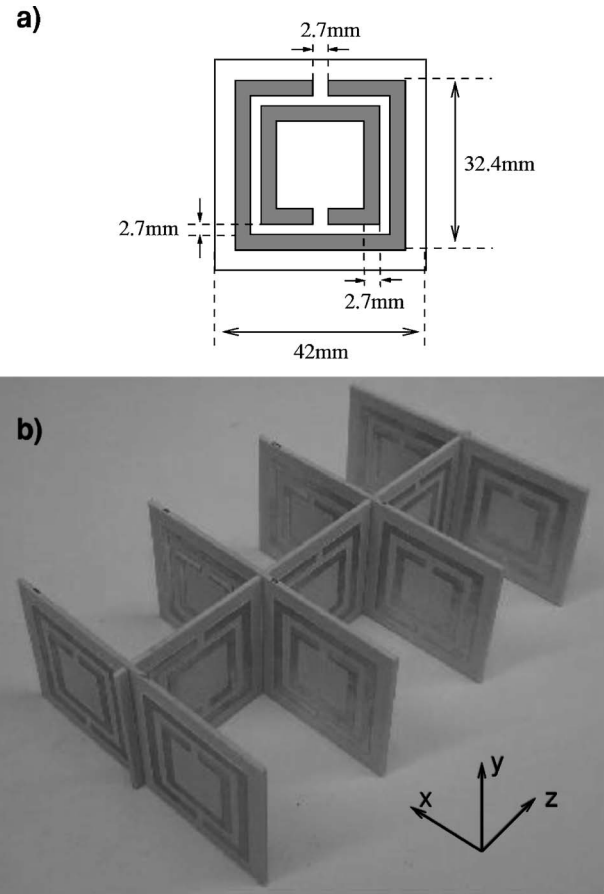


FIG. 3. (a) Split ring resonator geometry; (b) photograph of the SRR metamaterial.

metamaterial is also shown in the top of Fig. 4. We used an HP8720C vector network analyzer to measure the fields at frequencies between 800 and 900 MHz. Based on theoretical analysis, the fields are closest to ideal evanescent enhancement at the frequency where the ratio of the field amplitudes at the second and first material interfaces is a maximum. This occurred at 811.39 MHz, corresponding to a free space wavelength of 370 mm.

At this frequency, Fig. 4 shows the field distribution, amplitude, and phase, when the  $0.32\lambda$  long metamaterial was positioned inside the waveguide (red solid line) and, for reference, when the waveguide was empty (black dashed line). In the latter case, we were only able to measure the fields in the proximity of the source because, away from it, the amplitude decreased below the noise threshold of the network analyzer of  $-70$  dBm. The measurements marked with a circle in Fig. 4 are close to the noise threshold and may be less reliable, but they still show the expected decrease of the field amplitude.

With the metamaterial inside the waveguide, the field amplitude is strongly enhanced compared to the fields inside the empty waveguide. The measured field distribution also closely follows the theoretical prediction of exponential decay with a loss-induced enhancement at the first interface, then exponential growth, and finally exponential decay. The decay rate in the third, air-filled region ( $z > 0$ ) matches that of the  $TE_{10}$  mode, indicating that our SRR material has an

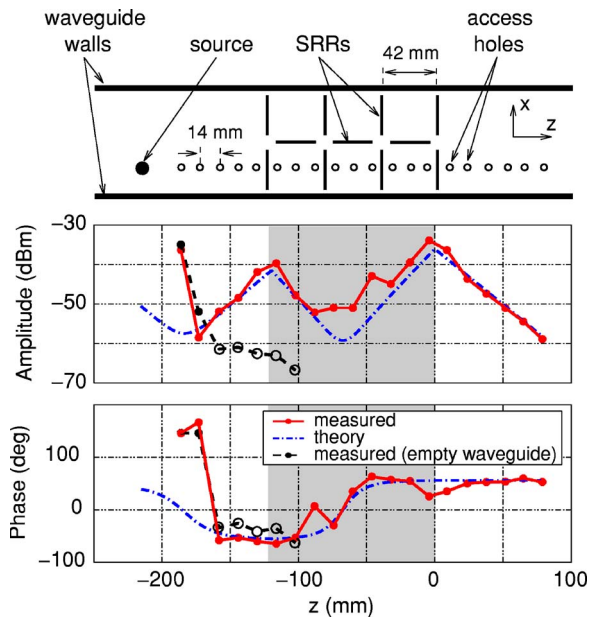


FIG. 4. (Color online) Top: a schematic, top view of the waveguide that highlights the position of the slab relative to the source and the access holes (i.e., the measurement points). Bottom: the field (amplitude and phase) measured inside these access holes. The match with the theoretical curve takes into account that the fields measured outside the slab have to closely match the theoretical ones.

effective permeability  $\mu$  close to the optimal permeability  $\mu_{\text{opt}}$ , which produces  $TE_{10}$  evanescent mode enhancement. It has been shown in both simulations [15] and experiments [11] that the effective material parameters can be found reliably by matching the measured fields with the analytically derived ones. In this case, we use the theoretical fields given by Eqs. (1)–(3) and the following matching procedure to find the effective permeability.

For different values of  $\varepsilon$  above  $\varepsilon_0$ , we computed  $\mu_{\text{opt}}$  using Eq. (6). We iteratively compared the measured fields to those computed theoretically using Eqs. (1)–(3) for different values of  $\mu$  around  $\mu_{\text{opt}}$ . The best match was obtained for  $\varepsilon = \varepsilon_0$  ( $\mu_{\text{opt}} = -1.2767\mu_0$  at 811.39 MHz), and  $\mu = (-1.2807 - j0.01)\mu_0$ , which is within 0.5% of  $\mu_{\text{opt}}$ . The field distribution for these values of  $\varepsilon$  and  $\mu$  is given in Fig. 4 (the blue dot-dashed line). Since the theoretical amplitude varies exponentially with  $\mu$  and  $\varepsilon$ , we expect the determined values of

$\mu$  and  $\varepsilon$  to be close to the real effective parameters. Indeed, deviations of  $<1\%$  from these values produced a clear mismatch between measurements and theoretical fields (not shown). Note that the fields near the source are the same with and without the SRR slab; thus, the slab does not modify the  $TE_{10}$  mode excitation. The fields near the source wire have a complicated spatial distribution that we attribute to multi-mode excitation. But for  $z > -160$  mm, these higher order modes have decayed and only the enhanced  $TE_{10}$  mode fields remain. In this region, we are able to obtain good agreement between theory and measurement.

The fields inside the metamaterial follow the theoretically expected shape inside a homogeneous material, with a 5–10 dB increase in amplitude that we attribute to the highly inhomogeneous quasistatic fields in the proximity of the SRRs. Simulations of the same structure performed with HFSS, a finite element solver of Maxwell’s equations, show field enhancements near the edges of the SRRs very similar to those measured adjacent to the SRRs at  $z = -42$  mm and  $z = -84$  mm.

Figure 4 allows us to quantify the ability of our metamaterial to recover the  $TE_{10}$  mode. Assuming that the amplitude of this mode at the source is that predicted theoretically (i.e., around  $-50$  dBm), we note that the amplitude becomes  $-50$  dBm again 266 mm away from the source (i.e., at  $z = 51$  mm). In other words, the 126 mm metamaterial slab canceled the decay of the  $TE_{10}$  mode on  $d_{\text{air}} = 140$  mm in the air-filled region (both in front and behind the metamaterial). The negative permeability slab thus enhances the  $TE_{10}$  mode field by 74 dB above the amplitude without the slab. The resolution enhancement (as defined in Ref. [9]) is at least  $k_{10}/k_0 = 2.15$ .

In conclusion, we showed theoretically how a passive material with negative permeability can produce the same evanescent wave enhancement as a true  $n = -1$  material for one transverse number. Implementing this experimentally in an rf waveguide experiment with a SRR-based metamaterial, we showed that field measurements inside this metamaterial demonstrate 74 dB of evanescent wave enhancement. The magnitude of this enhancement and, more importantly, the spatial variation of the fields are in close agreement with theoretical predictions, confirming the behavior of evanescent waves in a finite NIM slab (and connected subwavelength focusing) predicted by Pendry [1].

This work was supported by DARPA through Contract No. HR001-05-C-0068.

[1] J. B. Pendry, Phys. Rev. Lett. **85**, 3966 (2000).  
 [2] V. G. Veselago, Sov. Phys. Usp. **10**, 509 (1968).  
 [3] R. A. Shelby, D. R. Smith, and S. Schultz, Science **292**, 77 (2001).  
 [4] A. A. Houck, J. B. Brock, and I. L. Chuang, Phys. Rev. Lett. **90**, 137401 (2003).  
 [5] A. Grbic and G. V. Eleftheriades, Phys. Rev. Lett. **92**, 117403 (2004).  
 [6] Nicholas Fang, Hyesog Lee, Cheng Sun, and Xiang Zhang,

Science **308**, 534 (2005).  
 [7] J. D. Baena, L. Jelinek, R. Marques, and F. Medina, Phys. Rev. B **72**, 075116 (2005).  
 [8] J. B. Pendry, A. J. Holden, D. J. Robbins, and W. J. Stewart, IEEE Trans. Microwave Theory Tech. **47**, 2075 (1999).  
 [9] D. R. Smith, D. Schurig, M. Rosenbluth, S. Schultz, S. A. Ramakrishna, and J. B. Pendry, Appl. Phys. Lett. **82**, 1506 (2003).  
 [10] J. T. Shen and P. M. Platzman, Appl. Phys. Lett. **80**, 3286

- (2002).
- [11] S. A. Cummer and B. I. Popa, *Appl. Phys. Lett.* **85**, 4564 (2004).
- [12] T. Koschny, M. Kafesaki, E. N. Economou, and C. M. Soukoulis, *Phys. Rev. Lett.* **93**, 107402 (2004).
- [13] D. M. Pozar, *Microwave Engineering* (Adison-Wesley, Reading, MA, 1990), pp. 259–266.
- [14] U. S. Inan and A. S. Inan, *Electromagnetic Waves* (Prentice-Hall, Englewood Cliffs, NJ, 2000), pp. 142–144.
- [15] B. I. Popa and S. A. Cummer, *Phys. Rev. B* **72**, 165102 (2005).